

Luminescent Iridium(III)-Terpyridine Complexes – Interplay of Ligand Centred and Charge Transfer States

Lucia Flamigni,^{*[a]} Barbara Ventura,^[a] Francesco Barigelletti,^{*[a]} Etienne Baranoff,^[b] Jean-Paul Collin,^{*[b]} and Jean-Pierre Sauvage^{*[b]}

Keywords: Iridium / Photochemistry / Luminescence / Charge transfer / Electron transfer

Electrochemical properties, ground state absorption spectra, luminescence spectra and lifetimes (at room temperature and 77 K) as well as transient absorption spectra are reported herein for newly synthesized iridium(III) complexes in which benzamide units are appended to the coordinated terpyridine fragments. The nature of the luminescent excited states ($\Phi < 2 \times 10^{-3}$ and τ in the microsecond range, in air-equilibrated acetonitrile at 298 K) is discussed with regards to the ligand-centred (³LC) or charge transfer (³CT) nature. At room temperature, the excited state, a predominantly ligand-centred triplet (³LC) for the iridium(III) terpyridine com-

pounds, is switched for the benzamide-containing complexes to a charge transfer state (³CT). Intense absorption in the visible range, high energy content, long excited states lifetimes at 298 and 77 K and good luminescence yields make these complexes very promising as photosensitisers (P). The CT nature of the excited states of the benzamide-containing complexes makes them ideal components for the construction of rigid, linear arrays of the Donor-P-Acceptor type for charge separation.

(© Wiley-VCH Verlag GmbH & Co. KGaA, 69451 Weinheim, Germany, 2005)

Introduction

Iridium(III) complexes of polypyridine ligands are increasingly being employed in relevant applications.^[1–5] For iridium(III) terpyridine (2,2':6',2''-terpyridine, tpy) complexes some interesting perspectives concern their use as biological labelling reagents^[6] as well as the building up of dyads and triads as models for photoenergy conversion schemes.^[7–9] [Ir(tpy)₂]³⁺ and derivatives like those of the Ir(ttpy)₂³⁺ family (ttpy = 4'-tolyl-tpy) exhibit favourable optical properties which include intense luminescence ($\Phi \approx 10^{-2}$) and lifetimes in the μ s time range.^[10] Furthermore, the luminescent levels for these complexes come at ca. 2.5 eV so that they have potential to act as efficient photosensitisers. Indeed, the possibility of developing linear arrays by attaching suitable groups at the 4'-position of tpy groups coordinated at the Ir^{III} ion is very appealing.^[8,9,11] The use of geometrically opposite photoactive and electroactive units (e.g. D and A, electron donor and acceptor units, respectively) has proven to be of importance within energy con-

version schemes.^[7] So far, the [Ir(tpy)₂]³⁺ unit integrated within linear triad arrays has been used both as an electron relay^[8a] and as a photosensitiser.^[9] Whereas it has proven to be rather effective as an electron relay, its properties as a photosensitiser (P) are less satisfactory. For this latter role, in fact, in dyads (D-P and P-A) and triads (D-P-A) designed to perform photoinduced charge separation, it is relevant to gain control over the early events triggered by light absorption at P. In fact, primary formation of the lowest-lying charge transfer (CT) states within P could favour subsequent intercomponent hole and electron migration towards the D and A interacting partners, once the thermodynamic requirements are met. In contrast, for ligand centred (LC) excited states, holes and electrons reside in physically coincident sites and the expected intercomponent charge shift steps could be slowed down and be less competitive towards other processes, e.g. energy transfer.^[9]

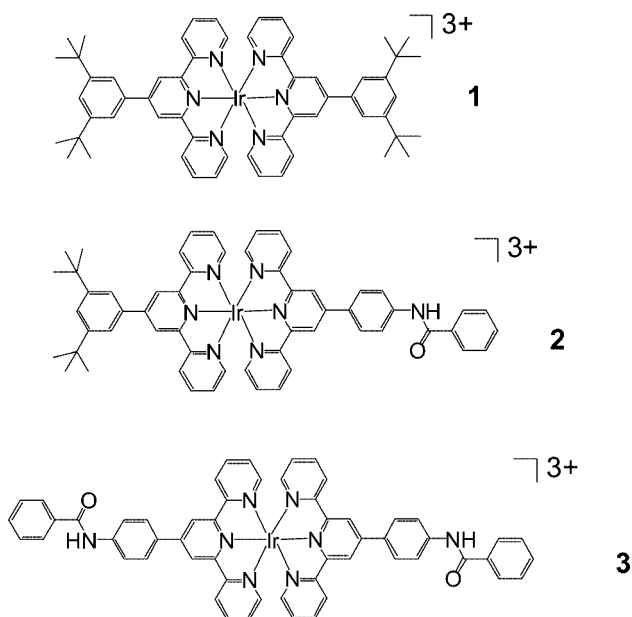
For the iridium(III) complexes of tpy derivatives studied up to now, the luminescent state has been found to be predominantly ligand centred, ³LC.^[10,11,13,14] This is in contrast to what happens for the closely investigated polypyridine complexes of transition metals such as ruthenium(II), osmium(II) and rhenium(I)^[12] which are currently being employed as photosensitisers and the emitting states of which are triplet metal-to-ligand states (³MLCT) in nature. In only one case, a scarcely emissive excited state in a 4-amino-biphenyl-substituted Ir(tpy) reported by Williams et al. was attributed to an intraligand charge transfer state, ILCT, where the appended group acts as a donor and the metal-

[a] Istituto ISOF-CNR,
Via P. Gobetti 101, 40129 Bologna, Italy
Fax: +39-051-639-9844
E-mail: flamigni@isof.cnr.it
franz@isof.cnr.it

[b] Laboratoire de Chimie Organo-Minérale, UMR 7513 CNRS,
Université Louis Pasteur, Institut Le Bel,
4, rue Blaise Pascal, 67070 Strasbourg, France
Fax: +33-390-241-368
E-mail: sauvage@chimie.u-strasbg.fr
jpcollin@chimie.u-strasbg.fr

bond terpyridyl unit behaves as an acceptor.^[11] The poor tendency of Ir(tpy) derivatives to form MLCT excited states can be understood on the basis of their electrochemical behaviour which is in contrast to that found for polypyridine complexes of transition metals such as ruthenium(II) and some others.^[12] For the latter complexes, the free energy for the reaction of the one-electron oxidised and reduced forms, $\Delta E_{1/2}$, correlates with the energy of the lowest-lying absorption and emission bands. These are MLCT in nature as evaluated from the longest-wavelength portions of absorption spectra (¹MLCT) and from the characteristics of the emission spectra (³MLCT).^[15] For instance, for [Ru(tpy)₂]²⁺, the metal centred oxidation, $E_{1/2}^{\text{ox}}$ (3+/2+), and the ligand centred reduction, $E_{1/2}^{\text{red}}$ (2+/-), are +1.30 and -1.24 V, respectively, with respect to the SCE in MeCN.^[16] The emission level, E_{em} , is ca. 2.0 eV so that $E_{\text{em}} \approx \Delta E_{1/2} - 0.5$ eV. On the other hand, for [Ir(tpy)₂]³⁺, $E_{1/2}^{\text{red}} = -0.77$ V but the oxidation of Ir(III) to Ir(IV) is not observed and $E_{1/2}^{\text{ox}} \geq +2.4$ V.^[10] Based on these electrochemical results and the above correlation, the ³MLCT level for [Ir(tpy)₂]³⁺ can be estimated higher (≥ 2.7 eV) than the luminescent ³LC level which is ca. 2.5 eV.^[11] It is worth mentioning here that a ligand-to-ligand excited state, LLCT, was identified as the emitting state in a related cyclometallated complex recently reported.^[17]

We show below that newly prepared Ir(III)-tpy type species with appended *N*-phenyl-benzamide fragments, **2** and **3** Scheme 1, also feature ³CT emission properties. Among other things, this CT character causes a low-energy shift of the main absorption bands in complexes **2** and **3** (bright yellow) in comparison with that observed in the prototype [Ir(tpy)₂]³⁺ complex or **1** (colourless or yellowish). This makes this series more promising for the conversion of solar light into chemical energy.



Scheme 1.

Results and Discussion

Synthesis and Electrochemistry

Complexes **1** and **2** were prepared as previously reported.^[8,10] Complex **3** was synthesized straightforwardly in one step from 4'-(benzamidophenyl)-2,2':6',2''-terpyridine (bap-tpy) and IrCl₃.

The redox characteristics of complexes **1**, **2** and **3** examined by cyclic voltammetry in acetonitrile (MeCN) are reported in Table 1. The working electrode used was a glassy carbon electrode since irreproducible and poorly defined signals were obtained with a platinum electrode due to adsorption phenomena. Two reversible ligand-centred^[10] one-electron waves followed by an irreversible peak at more negative potential were observed for the three complexes. As indicated by the values of the potentials, complex **1** is slightly more difficult to reduce than **2** and **3**. In fact, the presence of one (in **2**) or two (in **3**) benzamide groups leads to a very similar LUMO energy level in these two complexes. This fact is in agreement with the various spectroscopic properties observed for the three complexes (see below). Thus complex **1** has distinct characteristics compared with **2** and **3** which, in turn, are very similar to one another.

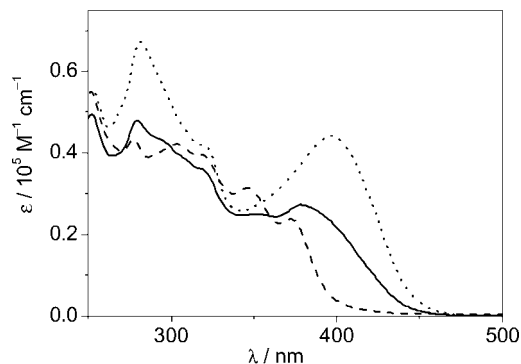
Table 1. Cyclic voltammetric data^[a] for the complexes **1**, **2** and **3**.

	$E_{1/2}$ (V vs. SCE)		
	tpy/tpy ⁻	tpy ⁻ /tpy ²⁻	tpy ²⁻ /tpy ³⁻
1	-0.79	-0.93	-1.80 ^[b]
2	-0.76	-0.92	-1.68 ^[b]
3	-0.76	-0.92	-1.65 ^[b]

[a] Solvent is MeCN, 0.1 M *n*Bu₄NPF₆ and SCE as the reference electrode ($v = 100$ mV s⁻¹). [b] Irreversible peak.

Optical Spectroscopy

Figure 1 shows the absorption spectra in MeCN solutions for the complexes shown in Scheme 1. For complex **1**, the absorption onset is at 400 nm and the UV features are due to intraligand ¹LC transitions as previously established.^[10] The spectra of complexes **2** and **3** are characterised by an additional, unstructured broad band extending

Figure 1. Absorption spectra in MeCN of **1** (dashed), **2** (solid) and **3** (dotted).

well beyond 400 nm. This band is about twice as intense in **3** as it is in **2** with $\epsilon_{398\text{nm}}$ ca. $45000 \text{ M}^{-1} \text{ cm}^{-1}$ and $\epsilon_{380\text{nm}}$ ca. $27000 \text{ M}^{-1} \text{ cm}^{-1}$, respectively (see Figure 1).

Figure 2 shows the room temperature luminescence spectra in air-free MeCN. In the inset, the luminescence decays at 298 K of **2** and **3** are also displayed. While a structured luminescence profile can be observed for **1** at 298 K, a broad unstructured band was recorded for both **2** and **3**. The luminescence lifetimes at room temperature of **2** and **3**, which are 800 and 1990 ns, respectively, are shorter than the lifetime of 6800 ns for **1**. The poor solubility of **2** and **3** limits the use of solvents with different dielectric constants which could be helpful in the assignment of the nature of the luminescent state at room temperature. A comparison of emission data in MeCN (dielectric constant = 36), methanol (dielectric constant = 33) and acetone (dielectric constant = 21) shows band maxima in the range 566–570 nm and does not provide any clear evidence of the effect of solvent polarity on the luminescent state energy levels.

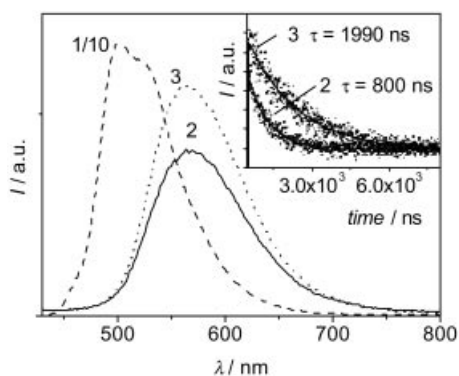


Figure 2. Corrected luminescence spectra ($\lambda_{\text{exc}} = 379 \text{ nm}$) at 298 K of optically matched solutions in air-free MeCN of **1** (dashed), **2** (solid) and **3** (dotted). In the inset the luminescence decay in air-free MeCN for **2** and **3** is reported with the exponential fitting.

In contrast to room temperature data, the luminescence spectra at 77 K in glassy butyronitrile (BuCN) illustrated in Figure 3 display rather similar spectroscopic profiles for **1**, **2** and **3**. The luminescence lifetimes detected at 77 K in BuCN for **2** and **3** are 80 and 85 μs , respectively, as shown in the insets of Figure 3. These are longer than the lifetime of 39 μs for **1** under the same conditions. Luminescence data in aerated and air-free MeCN at 298 K and in BuCN at 77 K are collected in Table 2. The room temperature reaction rate constants with oxygen (O_2 solubility in air equilibrated MeCN is $1.9 \times 10^{-3} \text{ M}^{[18]}$) can be derived from the lifetime data shown in Table 2 and are $2.5 \times 10^8 \text{ M}^{-1} \text{ s}^{-1}$, $4.2 \times 10^8 \text{ M}^{-1} \text{ s}^{-1}$ and $6.4 \times 10^8 \text{ M}^{-1} \text{ s}^{-1}$ for **1**, **2** and **3**, respectively, in agreement with previous reports.^[19]

We noticed that complexes **2** and **3** exhibit spectroscopic features, both in the low-energy regions of the absorption spectra and in the luminescence spectra at room temperature, which suggest an electronic nature other than neat LC for the excited states involved in the concerned transitions. Thus, the absorption profile for these complexes, see Figure 1, is characterised by a broad, unstructured band extending beyond 400 nm with ϵ_{max} of the order of

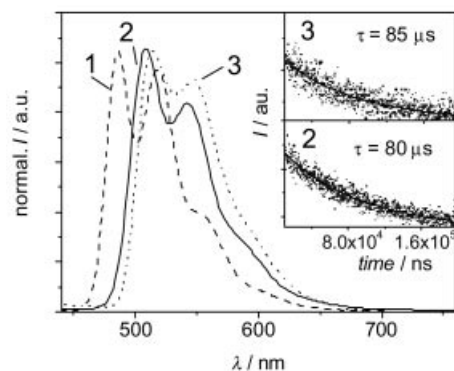


Figure 3. Normalised luminescence at 77 K in BuCN of **1** (dashed), **2** (solid) and **3** (dotted). In the inset the luminescence decay at 77 K in BuCN for **2** and **3** is reported with the exponential fitting.

Table 2. Luminescence data^[a] for the complexes **1**, **2** and **3**.

	298 K					77 K		$E_0^{[d]}$ eV	$HS^{[e]}$ cm^{-1}
	λ_{max} nm	$\Phi^{[b]}$ $\times 10^2$	$\tau^{[b]}$ ns	$\Phi^{[c]}$ $\times 10^2$	$\tau^{[c]}$ ns	λ_{max} nm	τ μs		
1	506	9.3	6800	2.2	1600	486	39	2.55	810
2	570	0.55	800	0.21	490	510	80	2.43	2060
3	566	0.76	1990	0.27	580	514	85	2.41	1790

[a] Solvent is MeCN at room temperature, BuCN at 77 K; excitation performed at 379 and 373 nm for the luminescence spectra and lifetimes, respectively. [b] Air-free MeCN. [c] Air-equilibrated MeCN. [d] Estimated energy content of the emitting level from the energy of the emission maximum at 77 K. [e] Hypsochromic shift for the emission band maximum on going from 298 to 77 K.

$10^4 \text{ M}^{-1} \text{ cm}^{-1}$. These absorption features are consistent with a CT character for the implied electronic transitions. From the luminescence properties of the complexes at room temperature, further indications about the CT nature of the luminescent state can similarly be drawn, as discussed below.

The room temperature luminescence spectroscopic profiles of complexes **2** and **3** look fairly unstructured as opposed to that of complex **1**, Figure 2. For the latter complex, the extended conjugation at the phenyl-tyl ligand coupled with nuclear rearrangements at the torsional angle between the aromatic rings^[20] is known to affect the spectroscopic profile.^[10,11] For complexes **2** and **3**, therefore, it seems that further electronic effects must be taken into account. With regard to the low-temperature results, complex **1** on one hand and **2** and **3** on the other hand exhibit different behaviour in terms of the hypsochromic shift (HS) on going from fluid (298 K) to frozen (77 K) solvent, Table 2. Actually, HS amounts to 810 cm^{-1} for **1** but 2060 and 1790 cm^{-1} for **2** and **3**, respectively. The difference between the luminescence profiles of **1**, **2** and **3** recorded in frozen solvents appears less important (Figure 3) but some difference in peak positions and luminescence lifetimes still appears.

Inspection of Table 2 confirms that the luminescent behaviour of **1** at room temperature is different from that of **2** and **3**. Actually, the luminescence lifetimes at room temperature of **2** and **3**, which are 800 and 1990 ns, respectively, (O_2 -free case) are well shorter than the lifetime of 6800 ns

for **1** but still quite remarkable in comparison with other transition metal complexes widely used for light energy conversion, being of the same order of magnitude or greater than the prototype complex [Ru(bpy)₃]²⁺.^[21] The luminescence quantum yield, Φ (Table 2, room temperature, O₂-free) for **1** is one order of magnitude larger than for **2** and **3**. Furthermore, use of Φ and τ values from Table 2 yields radiative rate constants k_r of $1.4 \times 10^4 \text{ s}^{-1}$ for **1** (for [Ir(tpy)₂]³⁺, k_r is 2.5×10^4)^[10] and ca. $5 \times 10^3 \text{ s}^{-1}$ for **2** and **3**. This also points to a different nature for the emissive state at room temperature. Based on all these observations, we ascribe the luminescence of **2** and **3** to an excited state with CT character.

An assessment of the nature of the excited states responsible for the luminescence and the type of vibrations affecting their deactivation can further be obtained by studying the luminescence spectroscopic profiles in terms of Franck–Condon envelopes.^[22–27] According to Equation (1a,b)^[22–23] (see Experimental Section), vibronic analyses for complexes **1**, **2** and **3** reveal similarities and differences between them. Figure 4 provides a direct comparison of results obtained both at room temperature and at 77 K. Derived estimates for the indicated parameters are further listed in Table 3 (for **1**, at room temperature, no satisfactory analysis could be applied). The luminescence profiles at 77 K for **1**, **2** and **3** exhibit the same vibrational progression, with a frequency $\hbar\omega_v$ in the range 1200–1280 cm⁻¹, Table 3. The displacement parameter along this frequency, S , was found to be 0.90, 0.75 and 0.84 for **1**, **2** and **3**, respectively. The 0–0 energy of the luminescent level, E_0 , is $\approx 2.8 \text{ eV}$ for **1** and $\approx 2.7 \text{ eV}$ for both **2** and **3**. This indicates that at 77 K, the luminescent state is deactivated via coupling with the same type of vibrational modes, which are likely to be C–N or C–C skeleton vibrations,^[24–27] with a similar extent of electronic delocalisation for all three cases. According to previous assignments for the ³LC emission for **1**,^[1,10,11] this suggests that at 77 K the nature of the emitting state in **2** and **3** is likewise ³LC.

With regards to the room temperature cases, analysis of the broad and unstructured luminescence shape for complexes **2** and **3** (Figure 4 and Table 3) yields a displacement parameter $S > 2$, supporting the view of a quite localised emitting level, with a coupled vibration $\hbar\omega_v \approx 600\text{--}700 \text{ cm}^{-1}$. Because of their CT character, on passing from room temperature to the frozen solvent (77 K), these levels can be expected to be highly destabilised which explains why the luminescence of **2** and **3** in the glass has ³LC origin, as for **1** (see Figure 4). This is supported by the large HS observed for **2** and **3** against a much smaller one for **1** on passing from room temperature to 77 K. We notice that the room temperature luminescence spectrum for **1** was not amenable to a profile analysis which might be explained by a *mixed* nature for the emission (presumably LC-CT) of this complex at this temperature.

Other interesting spectroscopic features which help to define useful spectroscopic differences among the investigated complexes are the excited state absorption spectra (ESA). Figure 5 shows the end of pulse spectra determined with

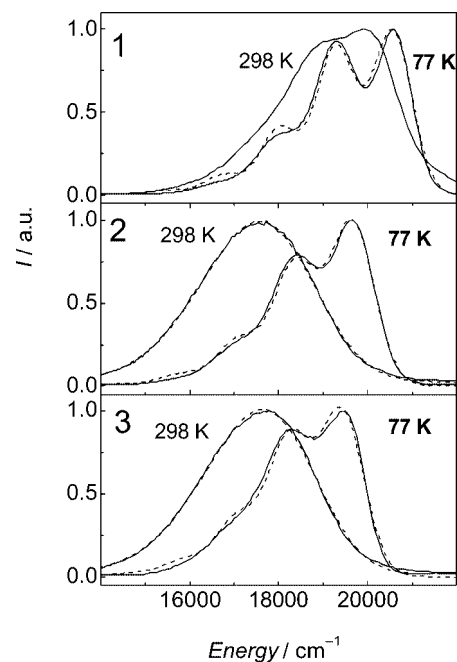


Figure 4. Vibronic analysis [dashed line, Equation (1a,b) of Experimental Section] of the corrected luminescence profiles (full line, an energy scale is employed) of complexes **1**, **2** and **3** as obtained in MeCN (room temperature) and BuCN (77 K); excitation was at 379 nm. For **1** at room temperature, the fit of the experimental profile was unsuccessful.

Table 3. Data from vibronic analyses of the luminescence spectra.^[a]

	298 K		77 K		
	2	3	1	2	3
$\hbar\omega_v$ [cm ⁻¹]	610	700	1270	1275	1190
λ_v [cm ⁻¹]	1580	1450	1140	960	1000
λ_s [cm ⁻¹]	1720	1430	1830	2270	2210
E_0 [eV]	2.57	2.52	2.78	2.72	2.69
S ^[b]	2.59	2.07	0.90	0.75	0.84

[a] According to Equation (1a,b) in the Experimental Section.^[22,23] Solvent: MeCN at room temperature, BuCN at 77 K; excitation performed at 379 nm. The room temperature spectra of **1** could not be analysed. [b] Displacement parameter, $S = \lambda_v/\hbar\omega_v$, see text.

picosecond resolution upon excitation with a 355 nm laser pulse of the complexes in air-equilibrated MeCN. The ESA profiles are quite different. Complex **1** shows a peak at 670 nm whereas both **2** and **3** display more intense and broad bands peaking at 780 nm. This is indicative of the fact that excited states of a different nature are involved in the transitions of **1** on one hand and **2** and **3** on the other, i.e. a ³LC state is involved in **1** and a ³CT in is involved in both **2** and **3**. The time evolution of the transient absorption in aerated and air-free solutions, as determined by a nanosecond flash photolysis experiment for **2** and **3**, is reported in Figure 6. The decay has a lifetime of 440 ns in air-equilibrated and 740 ns in air-free solutions for **2** and 530 ns in air-equilibrated and 1.75 μs in air-free solutions for **3**. The good agreement^[28] with the luminescence lifetimes indicates that the states responsible for the absorption are the same as those displaying luminescence. The molar

absorption coefficient of the triplet state for **2** and **3** was determined against a benzophenone in benzene actinometer (see experimental section for details) and $\epsilon_{780\text{nm}}$ was of the order of $15\,000\text{ M}^{-1}\text{ cm}^{-1}$. The characteristic and very strong ESA feature for **2** and **3**, in a spectroscopic region free from the absorbance of most D and A components, will prove very useful as a spectroscopic fingerprint during the study of the sequential events in the D-P-A arrays currently being designed.

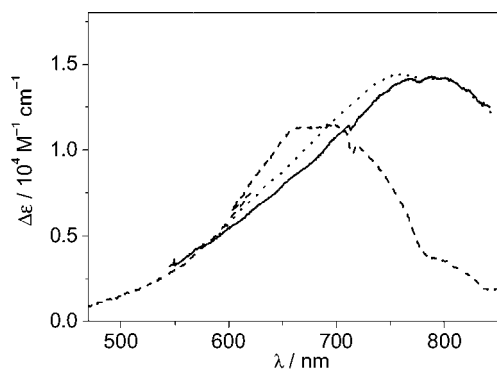


Figure 5. Excited state absorption spectra detected at the end of a laser pulse (35 ps, 355 nm, 3.5 mJ per pulse) in MeCN solutions. Symbols are: **1** (dashed), **2** (solid) and **3** (dotted).

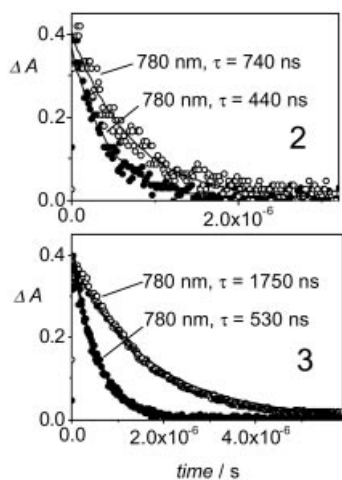


Figure 6. Time decay of excited state absorption spectra (full line results from exponential fit) detected at $\lambda = 780\text{ nm}$ in air-free (o) and air-equilibrated (●) optically matched solutions of **2** (upper panel) and **3** (lower panel) in MeCN following nanosecond laser excitation (18 ns, 355 nm, 1.9 mJ per pulse)

All the above observations are consistent with a predominantly ^3LC -type emission for **1** whereas **2** and **3** qualify better at room temperature as ^3CT emitters. The differences between **1** on the one hand and **2** and **3** on the other tend to disappear at 77 K, indicating a common nature for the emitting states in frozen solutions. This can be easily understood if one keeps in mind that the rigid environment, which prevents molecular reorientation, effectively destabilises CT states whereas this effect is only minor for LC states. In fact, our results suggest that at 77 K the three complexes exhibit an LC emission. In this respect, the lower and lower energy of emission at 77 K upon passing from **1**

to **2** and **3** could reflect a stabilisation induced by an increased delocalisation within the LC manifold.

While it is somewhat tempting to identify the CT state as a metal-to-ligand charge transfer, MLCT, in analogy to other photo- and electro-active transition metal complexes,^[12] an ILCT state should in fact also be considered. An ILCT state with the appended benzamide group acting as a donor while the metal-bond terpyridyl unit functions as an acceptor, similar to that postulated by Williams et al. for a 4-aminobiphenyl-substituted Ir(tpy)₂ complex,^[11] appears unlikely given the electrochemical inertness of the benzamide group which is rather difficult to oxidise.^[29] Another possible source of an ILCT excited state could be connected with the intrinsic properties of the ligand, in particular of the benzamide unit. It is therefore useful to recall the spectroscopic properties of *N*-phenylbenzamide. The latter material has been investigated by Lewis et al. in aromatic solvents and at room temperature it displays dual fluorescence which can be assigned to an $^1\text{n}-\pi^*$ transition ($\lambda_{\text{max}} = 433\text{ nm}$) and a twisted intramolecular charge transfer state, $^1\text{TICT}$ ($\lambda_{\text{max}} = 510\text{ nm}$), originating from a relaxed, higher energy $^1\pi-\pi^*$ state.^[30,31] The extended conjugation at the ligand, which occurs when benzamide units are appended to the tpy fragment coordinated to the metal centre, and the polar solvent could further stabilise the latter state so as to match the detected luminescent level in the present complexes. Accordingly, the low-lying CT transitions detected in the benzamide appended complexes **2** and **3** could be intra-ligand charge transfer in nature ($^3\text{ILCT}$) and localised on the *N*-phenyl benzamide fragment. This hypothesis, however, cannot explain the extremely large bathochromic shift, from 265 nm to ca. 400 nm, in the low energy absorption bands detected in these complexes with respect to *N*-phenylbenzamide.

So it seems that Ir^{III} to pab-tpy MLCT transitions could better explain the observed spectroscopic behaviour. However, we lack support from the electrochemistry for the occurrence of such CT transitions at low energy. As discussed above, with reference to the redox properties of [Ir(tpy)₂]³⁺, estimated levels for an Ir^{III} → L CT emission could be too high in energy in comparison with experimental findings. Nonetheless, the estimated energy gap between $^3\text{MLCT}$ and luminescent levels is not exceedingly large and thermal redistribution might well mix some $^3\text{MLCT}$ character into the luminescent level at room temperature.

Conclusions

New Ir^{III}-bisterpyridine type complexes exhibiting a low-lying excited state with ^3CT nature at room temperature have been synthesized and spectroscopically characterised. The lifetimes of the excited states of these complexes are long, $\tau \approx 1\text{--}2\ \mu\text{s}$, given the CT nature of the excited species. In a rigid matrix at 77 K the emission, which is ^3LC in character, exhibits lifetimes $\tau \approx 10^2\ \mu\text{s}$ which is longer than recorded for other [Ir(tpy)₂]³⁺ derivatives. In addition, with respect to previously investigated Ir^{III}-tpy type complexes,

complex **2** and, even more, complex **3** feature an absorption spectrum the lowest-energy portion of which is shifted towards the visible region of the spectrum and is characterised by a high molar absorption coefficient. Because of their spectroscopic and photophysical properties, complexes **2** and **3** appear promising as photosensitisers and assembling units in D-P-A arrays designed for exploring photoinduced charge separation. In fact, they combine an advantageous geometry which allows the construction of linear and rigid arrays with the presence of a CT excited state (at room temperature) which, being characterised by a separation of charges with respect to an LC excited state, is much better suited to initiate a multistep electron transfer required to achieve charge separation over long distances.

Experimental Section

The syntheses and characterisations of **1** and **2** have been reported elsewhere.^[8,10] Complex **3** was synthesized according to the following procedure: IrCl₃ and two equiv. of bap-tpy were heated at 196 °C in degassed ethylene glycol in the dark for 20 min. After precipitation with an aqueous solution of KPF₆, crude **3** was purified by column chromatography (silica, CH₃CN / water / saturated KNO₃ solution 100:10:1) to give **3** in 40% yield as a yellow solid. ¹H NMR (CD₃CN, 300 MHz): δ = 9.17 (s, 2H, NH), 9.09 (s, 4H, H_{3'5'}), 8.73 (d, ³J = 7.5 Hz, 4H, H_{33''}), 8.27 (d, ³J = 8.9 Hz, 4H, H₀₁), 8.25 (m, 4H, H_{44''}), 8.18 (d, ³J = 8.9 Hz, 4H, H_{m2}), 8.04 (d, ³J = 8.9 Hz, 4H, H₀₂), 7.72 (d, ³J = 8.8 Hz, 4H, H_{66''}), 7.66–7.57 (m, 6H, H_{m2}, H_{p2}), 7.51 (ddd, ³J = 6.9 and ⁴J = 1.2 Hz, 4H, H_{55''}) ppm. ES-MS, *m/z* (calcd.): 349.75 (349.76) [M – 3PF₆]³⁺.

Spectrophotometric grade acetonitrile or butyronitrile solvents were used. Absorption and luminescence spectra were measured with a Perkin–Elmer Lambda 5 UV/Vis spectrophotometer and a Spex Fluorolog II spectrofluorimeter, respectively. Solutions were purged of air by bubbling with argon for 10 min. The samples were contained in home designed 10 mm fluorescence cells. Luminescence quantum yields (Φ) were evaluated, after correcting for the photomultiplier response, with reference to air-equilibrated [Ir(tpy)₂](PF₆)₃ in aerated acetonitrile as a standard ($\Phi = 0.029$).^[10] Luminescence lifetimes (τ) were obtained with an IBH single photon counting instrument upon excitation at 373 nm from a pulsed diode source. Transient absorption spectra were determined by a pump-probe spectrograph with 30 ps resolution based on a Nd-YAG laser (355 nm, 10 Hz).^[32] The lifetime of the absorbing excited state was determined by a laser flash photolysis system based on a Nd-YAG laser (355 nm, 18 ns pulse) previously described.^[33] Molar absorption coefficients of the excited states were determined with the same nanosecond apparatus using the benzophenone in benzene actinometer ($\lambda = 530$ nm, $\epsilon = 7\,220$ M⁻¹ cm⁻¹, $\Phi_T = 1$).^[34] The experimental uncertainty in the absorption and luminescence maxima is 2 nm. The uncertainties in the τ values and the Φ values are 10 and 20%, respectively.

The vibronic band profiles of the corrected luminescence spectra, $I(E)$, on an energy scale [E (cm⁻¹)] were analysed according to Equations (1a) and (1b) which describe the relation between the Frank–Condon envelope, $FC(E)$, and some other pertinent parameters.^[22–23]

$$I(E) = \text{const} \times FC(E) \quad (1a)$$

$$FC(E) = \sum_{j=0}^{\infty} F_j (4\pi\lambda_s k_B T)^{-1/2} \exp\left(-\frac{(E - E_0 + j\hbar\omega_v + \lambda_s)^2}{4\lambda_s k_B T}\right) \quad (1b)$$

$$\text{with } F_j = \exp(-S) \frac{S^j}{j!}; \text{ and } S = \frac{\lambda_v \dots}{\hbar\omega_v}$$

In this equation, E_0 is the energy of the 0–0 transition (the energy gap between the 0–0 vibrational levels in the excited and ground states), j is a vibrational quantum number for high-frequency modes, $\hbar\omega_v$ (in practice an upper limit $j = 5$ is taken into account), λ_v and λ_s are internal and solvent reorganisation parameters, S is a displacement parameter and k_B is the Boltzmann constant. A nonlinear least-squares fit of Equation (1a,b)^[35] to the experimental spectra provides estimates for E_0 , λ_v , λ_s and the displacement parameter S along the $\hbar\omega_v$ vibrational mode (predominantly contributing to deactivation of the excited level). The magnitude of S (the electron-vibrational coupling constant or Huang–Rhys factor) is related to the relative intensities of the individual components in the vibrational progression. Analysis according to Equation (1a,b) allows, among other things, an assessment of the extent of delocalisation of the luminescent level which undergoes deactivation because of coupling with ground state $\hbar\omega_v$ vibrational modes. High values for S (typically in the range 0.7 to 1 and more)^[27] indicate that the excited state is significantly distorted along the concerned vibrational mode because of electronic localisation effects. On the contrary, when the excited state undergoes extended electronic delocalisation, low S values are obtained (typically in the range 0.2 to 0.6)^[24,36] indicating that the electronic curve for the excited level is not displaced much relative to that for the ground state.

Acknowledgments

We thank CNRS (France), CNR (Italy) and the Ministero dell'istruzione, dell'Università e della Ricerca of Italy (FIRB, RBNE019H9K) for financial support. E. B. acknowledge support from the French Ministry of Education. We thank also Johnson Matthey Inc. for a loan of IrCl₃.

- I. M. Dixon, J. P. Collin, J.-P. Sauvage, L. Flamigni, S. Encinas, F. Barigelletti, *Chem. Soc. Rev.* **2000**, *29*, 385–391.
- X. Gong, J. C. Ostrowski, G. C. Bazan, D. Moses, A. J. Heeger, M. S. Liu, A. K. Y. Jen, *Adv. Mater.* **2003**, *15*, 45–49.
- K. K. W. Lo, C. K. Chung, T. K. M. Lee, L. H. Lui, K. H. K. Tsang, N. Y. Zhu, *Inorg. Chem.* **2003**, *42*, 6886–6897.
- V. I. Adamovich, S. R. Cordero, P. I. Djurovich, A. Tamayo, M. E. Thompson, B. W. D'Andrade, S. R. Forrest, *Organic Electronics* **2003**, *4*, 77–87.
- M. A. Baldo, S. Lamansky, P. E. Burrows, M. E. Thompson, S. R. Forrest, *Appl. Phys. Lett.* **1999**, *75*, 4–6.
- a) K. K. W. Lo, C. K. Chung, D. C. M. Ng, N. Y. Zhu, *New J. Chem.* **2002**, *26*, 81–88; b) K. K. W. Lo, C. K. Chung, N. Y. Zhu, *Chem. Eur. J.* **2003**, *9*, 475–483.
- E. Baranoff, J.-P. Collin, J.-P. Sauvage, L. Flamigni, *Chem. Soc. Rev.* **2004**, *33*, 147–155.
- a) I. M. Dixon, J.-P. Collin, J.-P. Sauvage, L. Flamigni, *Inorg. Chem.* **2001**, *40*, 5507–5517; b) E. Baranoff, I. M. Dixon, J.-P. Collin, J.-P. Sauvage, B. Ventura, L. Flamigni, *Inorg. Chem.* **2004**, *43*, 3057–3066.
- L. Flamigni, G. Marconi, I. M. Dixon, J.-P. Collin, J.-P. Sauvage, *J. Phys. Chem. B* **2002**, *106*, 6663–6671.

- [10] J.-P. Collin, I. M. Dixon, J.-P. Sauvage, J. A. G. Williams, F. Barigelletti, L. Flamigni, *J. Am. Chem. Soc.* **1999**, *121*, 5009–5016.
- [11] W. Leslie, A. S. Batsanov, J. A. K. Howard, J. A. G. Williams, *Dalton Trans.* **2004**, 623–631.
- [12] V. Balzani, A. Juris, M. Venturi, S. Campagna, S. Serroni, *Chem. Rev.* **1996**, *96*, 759–834.
- [13] M. Licini, J. A. G. Williams, *Chem. Commun.* **1999**, 1943–1944.
- [14] W. Goodall, J. A. G. Williams, *J. Chem. Soc., Dalton Trans.* **2000**, 2893–2895.
- [15] A. A. Vlcek, E. S. Dodsworth, W. J. Pietro, A. B. P. Lever, *Inorg. Chem.* **1995**, *34*, 1906–1913.
- [16] J.-P. Sauvage, J.-P. Collin, J. C. Chambron, S. Guillerez, C. Codret, V. Balzani, F. Barigelletti, L. De Cola, L. Flamigni, *Chem. Rev.* **1994**, *94*, 993–1019.
- [17] M. Polson, S. Fracasso, V. Bertolasi, M. Ravaglia, F. Scandola, *Inorg. Chem.* **2004**, *43*, 1950–1956.
- [18] S. L. Murov, I. Carmichael, G. L. Hug, *Handbook of Photochemistry*, Marcel Dekker, New York, **1993**, p. 289, .
- [19] N. P. Ayala, C. M. Flynn, Jr., L. A. Sacksteder, J. N. Demas, B. A. DeGraff, *J. Am. Chem. Soc.* **1990**, *112*, 3837–3844.
- [20] Y. Kim, C. M. Lieber, *Inorg. Chem.* **1989**, *28*, 3990–3992.
- [21] A. Juris, V. Balzani, F. Barigelletti, S. Campagna, P. Belser, A. von Zelewsky, *Coord. Chem. Rev.* **1988**, *84*, 85.
- [22] I. R. Gould, S. Farid, *J. Photochem. Photobiol. A* **1992**, *65*, 133–147.
- [23] I. R. Gould, R. H. Young, R. E. Moody, S. Farid, *J. Phys. Chem.* **1991**, *95*, 2068–2080.
- [24] J. A. Treadway, G. F. Strouse, R. R. Ruminski, T. J. Meyer, *Inorg. Chem.* **2001**, *40*, 4508–4509.
- [25] J. P. Claude, T. J. Meyer, *J. Phys. Chem.* **1995**, *99*, 51–54.
- [26] Z. Murtaza, D. K. Graff, A. P. Zipp, L. A. Worl, W. E. Jones, W. D. Bates, T. J. Meyer, *J. Phys. Chem.* **1994**, *98*, 10504–10513.
- [27] E. M. Kober, J. V. Caspar, R. S. Lumpkin, T. J. Meyer, *J. Phys. Chem.* **1986**, *90*, 3722–3734.
- [28] It should be noticed that the absorbing species lifetimes detected by laser flash photolysis are, in general, shorter than those of the same luminescent species determined by single photon techniques. This is caused by the much higher photon flux which is used in laser flash photolysis experiments and this, increasing the concentration of excited states, introduces a second order component due to self annihilation in the decay which tends to shorten the lifetime compared with low intensity determinations.
- [29] No oxidation of the benzamide fragment was observed in a scan of the complexes up to 1.6 V vs. SCE.
- [30] D. D. Lewis, T. M. Long, *J. Phys. Chem. A* **1998**, *102*, 5327–5332.
- [31] F. D. Lewis, W. Z. Liu, *J. Phys. Chem. A* **1999**, *103*, 9678–9686.
- [32] L. Flamigni, N. Armaroli, F. Barigelletti, V. Balzani, J.-P. Collin, J.-O. Dalbavie, V. Heitz, J.-P. Sauvage, *J. Phys. Chem. B* **1997**, *101*, 5936–5943.
- [33] L. Flamigni, *J. Phys. Chem.* **1992**, *96*, 3331–3337.
- [34] S. L. Murov, I. Carmichael, G. L. Hug, *Handbook of Photochemistry*, Marcel Dekker, New York, **1993**, p. 107.
- [35] P. R. Bevington, *Data Reduction and Error Analysis for the Physical Sciences*, chapter 11, McGraw-Hill, New York, **1969**.
- [36] L. Hammarström, F. Barigelletti, L. Flamigni, M. T. Indelli, N. Armaroli, G. Calogero, M. Guardigli, A. Sour, J.-P. Collin, J.-P. Sauvage, *J. Phys. Chem. A* **1997**, *101*, 9061–9069.

Received: September 24, 2004